

5-2016

# Characterizing Kepler Objects of Interest Using the Algorithm EXONEST

Bertrand Carado

*University at Albany, State University of New York*

Follow this and additional works at: [https://scholarsarchive.library.albany.edu/honorscollege\\_physics](https://scholarsarchive.library.albany.edu/honorscollege_physics)



Part of the [Physics Commons](#)

---

## Recommended Citation

Carado, Bertrand, "Characterizing Kepler Objects of Interest Using the Algorithm EXONEST" (2016). *Physics*. 6.  
[https://scholarsarchive.library.albany.edu/honorscollege\\_physics/6](https://scholarsarchive.library.albany.edu/honorscollege_physics/6)

This Honors Thesis is brought to you for free and open access by the Honors College at Scholars Archive. It has been accepted for inclusion in Physics by an authorized administrator of Scholars Archive. For more information, please contact [scholarsarchive@albany.edu](mailto:scholarsarchive@albany.edu).

# Characterizing Kepler Objects of Interest Using the Algorithm EXONEST

An honors thesis presented to the  
Department of Physics,  
University at Albany, State University Of New York  
in partial fulfillment of the requirements  
for graduation with Honors in Physics  
and  
graduation from The Honors College.

Bertrand Carado

Research Advisor: Kevin H. Knuth, Ph.D.

April, 2016

The experience was truly visceral - shivers would run up and down my spine every time I pointed the telescope at a patch of stars. Eventually the feeling went away, but I still remember it. As I looked at the darkness between the stars, I felt as if I could fall into it. Like a fear of heights in reverse. Like an upside-down vertigo.

Dimitar Sasselov

Even with an early bedtime, in winter you could sometimes see the stars. I would look at them, twinkling and remote, and wonder what they were. I would ask older children and adults, who would only reply, "They're light in the sky, kid." I could see they were lights in the sky. But what were they? Just small hovering lamps? What for? I felt a kind of sorrow for them: a commonplace whose strangeness remained somehow hidden from my incurious fellows. There had to be some deeper answer.

Carl Sagan

Who has not felt a sense of awe while looking deep into the skies lit with countless stars on a clear night? Who has failed to wonder whether there is an intelligence behind the cosmos? Who has not asked themselves if ours is the only planet to support living creatures? To me, these are natural curiosities in the human mind.

His Holiness the Dalai Lama

La lumière des étoiles tombe doucement comme une pluie. Elle ne fait pas de bruit, elle ne soulève pas de poussière, elle ne creuse aucun vent.<sup>1</sup>

J.M.G. Le Clézio

## Abstract

Recent observations across the galaxy have led to the conclusion that there exist many different extrasolar systems. Using photometric effects, the amount of data that has been produced on exoplanets has significantly increased and will continue to rise. Finding new methods of data analysis to broaden the spectrum of research has therefore become a necessity. Exonest is an algorithm currently in development that uses Bayesian methods, and notably nested sampling, to infer characteristics about an exoplanet from its observed light curve.

In this paper, Exonest was tested by being used to study three extra-solar systems: each containing a single confirmed hot Jupiter (a large planet orbiting close to its host-star). The planets selected for this test were Kepler-428b, Kepler-40b, and Kepler-44b. Three parameters were computed and compared with the published values by NASA: the mass, the radius and the relative orbital inclination of the planet. The values returned by the algorithm are generally in agreement with NASA, which would tend to validate Exonest as a robust and powerful analysis tool. In the case of Kepler-428b, the dayside and nightside temperatures were also determined, although no other estimation of these parameters was available for comparison.

**Keywords:** Extrasolar planets, Astrometry, Data management.

PACS: 97.82.-j, 95.10.Jk, 07.05.Kf.

## Acknowledgment

I would like to acknowledge the profound and constant moral support of my parents. Without them, I would never have had the amazing opportunity to study in the United-States and to write this thesis. This work is the result of their constant love and affection. By being themselves very passionate about ideas, they contributed to foster my curiosity for culture in general and science in particular, since the beginning of my life. I am still amazed by the lively and engaging discussions I can have with them. Above everything, they offered me that precious time to become myself, and to dream. I still have much to learn, but it seems to me that being able to dream is an essential quality in any free human being.

Dr. Lunin, an amazing teacher, whose intellectual rigor allied to the most noble human qualities, had a profound impact on my interest for physics, along with Dr. Kuan and Dr. Landford. Dr. Knuth is an equally brilliant teacher whose breath of knowledge, spectrum of interests and eternal curiosity has never ceased to astound me. I will be forever grateful to him for giving me the opportunity to study Exoplanets, and thus fulfilling an old dream of mine to let my spirit travel among the stars, and to let my heart remain in this time which is between the seconds, at the border of eternity.

I am equally indebted to all the members of the exoplanet team, under the dynamic management of Dr. Knuth, especially Ms. Carter and Dr. Placek, for their constant help and support throughout my research.

I must also acknowledge the decisive impact of one of my high school physics teachers, Mr. David Duffour who communicated to me his genuine curiosity and amazement for this very curious and beautiful Universe and, and with his remarkable sensitivity and intelligence, has fostered my subsequent attachment to this equally curious and beautiful discipline that is Physics.

Finally, I will mention Ms. Yuchao Ma whose very name led me to believe that there is a World, indeed, beyond my Universe, and a future beyond the present.

## Table of Contents

Abstract.....	4
Acknowledgment.....	5
Introduction.....	7
What are exoplanets and why look for them?.....	9
How to find exoplanets? Overview of the photometric methods.....	12
Characterizing exoplanets: applying Bayes' theorem in the algorithm EXONEST.....	24
Using EXONEST to characterize Kepler-428b, 40b and 44b.....	27
Conclusion.....	33
References.....	35

## I. INTRODUCTION

The star Sirius was originally welcomed with great delight and relief by the ancient Egyptians, it announced the beginning of a new cycle, the return of the flooding where the Nile, taking its source and its strength from the high African plateaus, would cover the cultivated lands, rendering them fertile again. Sirius was associated with the goddess Sothis and her apparition in the sky was another victory of life over death, the promise of another new beginning, an eternal return<sup>2</sup>.

The immense dignity and restraint of the Egyptian art served only one purpose: to apprehend and access eternity. In an all changing world, where even the sand dunes were constantly shifting under the wind, the Egyptians naturally turned their gaze toward the night sky in search for stillness and peace, and contemplated in wonder the body of the goddess Nut. The Milky Way was the shape of her naked body and the stars, her adornments<sup>2</sup>. The most beautiful myths and the greatest spiritual achievements have revolved around the sky illuminated by countless stars. With the advent of philosophy and logic, Democritus, born in northern Greece, with his remarkable sense of intuition mixed to an uncanny imagination, was the first to suggest the existence of other worlds, around the 4<sup>th</sup> century B.C, possibly inhabited<sup>3</sup>.

However, with the triumph of the Aristotelian model and philosophy, the Western world inherited an anthropocentric view for the millennium to come. It was not until the sixteenth century, with Giordano Bruno, that new controversial ideas started to arise. As a follower of the Copernican view, Bruno saw no reason why the planets revolving around the Sun should be taken as everything and why the Universe itself should not be infinite<sup>4</sup>. Isaac Newton later advanced that the physical and gravitational architecture of the solar system could very well be repeated around other stars<sup>5</sup>.

With the achievements of modern science, and the improvement of radio-telescopes, the first real proof of the existence of worlds beyond the limit of the solar system came around 1992 with the discovery of two planets orbiting the pulsar PSR 1257+12, approximately 1000 light years away from the Earth<sup>6</sup>. The first exoplanet orbiting a main-sequence star, 51 Pe-



gasi b, orbiting the Sun-like 51 Pegasi in the constellation of Pegasus was discovered<sup>7</sup> in 1995.

Unfortunately, the disturbance of incoming electromagnetic radiation through the atmosphere (astronomical scintillation or twinkling: causing variations in apparent brightness<sup>8</sup>) and the ever increasing light pollution on Earth, has rendered the use of telescopes relatively limited for the search of exoplanets. The sending of observatories directly into space, where the observational issues mentioned above are irrelevant, has therefore become a popular choice. It has culminated so far in the launch by NASA on March 7, 2009, of the Kepler spacecraft<sup>9</sup>. This observatory is relatively simple and consists of one single instrument: a very sophisticated and extremely sensitive photometer (measuring light intensity) and was specifically designed to probe the light of over 150,000 main sequence stars in order to find exoplanets<sup>9</sup>. Raw data is then transmitted to Earth for analysis. An artist's impression of Kepler is shown in Figure 1.



FIG. 1: Artist's view of the Kepler space telescope. (Image credit: Wendy Stenzel (2009). NASA, Kepler mission.)

It is interesting to note that Kepler surveys only a relatively small portion of the Milky-Way (as shown on Figure 2). From that specific region, extrapolations are made and corrected as new data becomes available to determine the possible total number of exoplanets in the galaxy<sup>10</sup>. The current estimation (however rough) places the number of terrestrial planets at over 10 billion<sup>10</sup>. Thanks to Kepler, as of February 2016, the existence of 1039 planets was confirmed, with the number of candidates being 4696<sup>11</sup>. Those numbers will of course be outdated very soon. However, it is interesting to notice that only 715 exoplanets had been discovered by the beginning of 2014<sup>12</sup>. What this shows is the quick and incredible improvement of detection and data analysis methods, and above all the surprising variety and number of extra-solar systems.

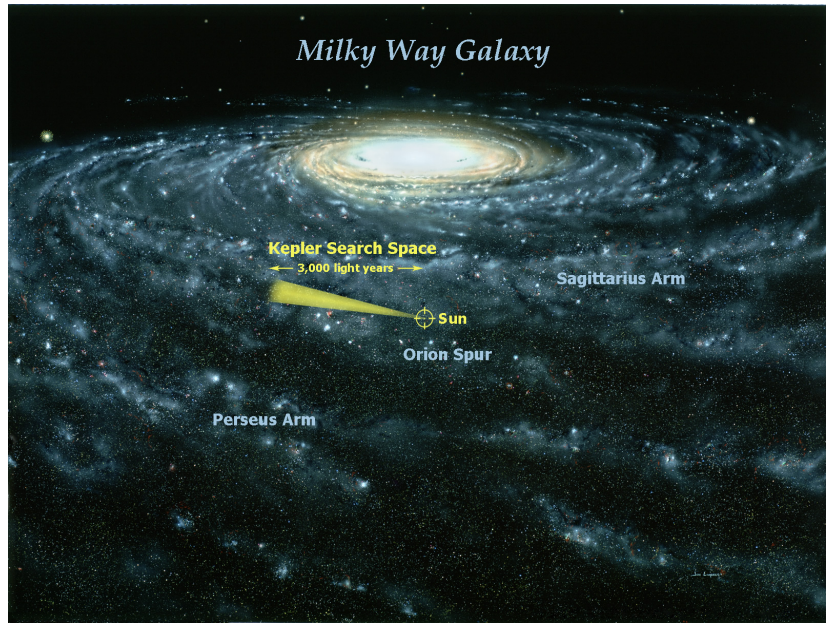


FIG. 2: Artist's view of the Kepler space telescope. (Image credit: Wendy Stenzel (2009). NASA, Kepler mission.)

## II. WHAT ARE EXOPLANETS AND WHY LOOK FOR THEM?

For the purpose of this thesis, an exoplanet (or extra-solar planet) is a planet that orbits a star which is not the Sun. Interestingly, the actual definition of the word “planet” is complex and subject to variations in literature<sup>13</sup>. It is not the purpose of this thesis to explore this problem. However, the usual convention should be mentioned: it designates an object that was formed around a star by “accretion of planetesimals in a circumstellar dust disk [...], just by analogy with Solar System planets”<sup>13</sup>.

How, then, is it possible to make a difference between planets and brown-dwarfs, which are “objects formed by collapse in a gas cloud or circumstellar disk [...], by analogy with stars”<sup>13</sup>? The answer lies in observations and theoretical notions “that make it plausible that the population below around 25 MJup [the mass of Jupiter] is essentially made of planets (in the above sense)”<sup>13</sup>. We are not concerned here with floating (or “rogue”) planet candidates.

Many discovered exoplanets were confirmed to be gas giants which are chiefly composed of light elements such as helium and hydrogen<sup>14</sup>. Alpha Centauri Bb could be the nearest exoplanet, if confirmed<sup>15</sup>. The least massive of them could be PSR B1257+12 A, which would have a mass approximately twice that of the moon<sup>16</sup>. DENIS-P J082303.1-491201 b would however be 29 times the mass of Jupiter<sup>17</sup> (it is thought to be a possible brown dwarf). Some planets orbit their host-star in a matter of hours; whereas some take thousands of years. Most of the exoplanets detected so far are in the Milky Way, but the existence of extragalactic planets was also confirmed<sup>18</sup>.

Of course, one of the greatest questions Humankind has asked itself over the course of the millenia, was about the possibility for other worlds and perhaps other civilizations to exist among the stars. While some of the oldest philosophies and religions on Earth are not intrinsically opposed to this idea, the anthropocentric view that dominated western civilization until quite recently has made the question all the more important. Even today, some people feel uncomfortable with the idea that human beings might be but a tiny fraction of the life in the Universe, and that the development of life itself is an uncertain, fragile and chaotic process. It became visible, for instance, in some controversial claims such as

those made by the Intelligent Design (ID) proponents, where life itself is viewed as the ultimate goal of the Universe<sup>19</sup>. Some of these pseudo-scientific arguments are used to bring human beings back to the center of the cosmos (reviving creationism), by notably saying that natural selection is not an undirected process<sup>20</sup>.

Even recent discoveries in anthropology have undermined those arguments by demonstrating the randomness of evolution (which should not prevent us from marveling at the outstanding creativity that nature has shown along the way), not exempting humankind<sup>21</sup>.

However, what this example shows is the incredible passion that exists around the question of our place in the immensity of the cosmos, and of our possible loneliness across the stars. Interestingly, exoplanets are now used in arguments and discussions, even in theoretical physics. The astronomer and mathematician Johann Kepler was asking himself why the Earth had to be 150 millions kilometers away from the Sun and sought to demonstrate that there had to be a deeper mathematical formulation behind that number<sup>22</sup>. Of course, this question today has become irrelevant as we look upon thousand of worlds, all of them with very different layouts. Using that argument, some scientists jump to the conclusion that the Universe itself must be but a tiny bubble in a vaster ensemble of independent Universes, which would explain why the fundamental constants of physics (for instance, the mass and charge of elementary particles) seem *a priori* so well adjusted for life to have appeared. To mathematically try to explain the peculiar “tuning” of those fundamental constants would therefore become irrelevant, as for Kepler trying to find a deeper meaning to the distance of the Earth from the Sun which was, in fact, an example among many others<sup>22</sup>.

The motivation behind the search for exoplanets revolves around finding the answer to one of the deepest questions asked by human beings. The challenge is to find planets that seem to share similar characteristics with Earth. The concept of the circumstellar habitable zone (CHZ) was hence developed since 1953 to answer this challenge<sup>23</sup>. The CHZ is a region around a star where a planet could potentially harbor liquid water and a biosphere similar to Earth. Of course, the habitable zone depends on the amount of radiant energy the planet receives from its host-star<sup>24</sup>. If the star is much colder (smaller in dimensions or dimmer) than the Sun, then the planet will have to be much closer to it, and conversely, it will have

to be much further away if the star is hotter (larger in dimensions or brighter).

In Figure 3, an example is given with the star Gliese 581 which is smaller than the Sun. Here the habitable zone is given as a function of the radius of the star compared to the radius of the Sun. Gliese 581c was discovered to have an orbit tangent to the habitable zone, but subsequent analysis of its atmosphere revealed that it was closer to Venus. Gliese 581d could be a potential candidate, the discovery of Gliese 581g (although shown as an example on Figure 3) was dis-confirmed in 2014<sup>25</sup>.

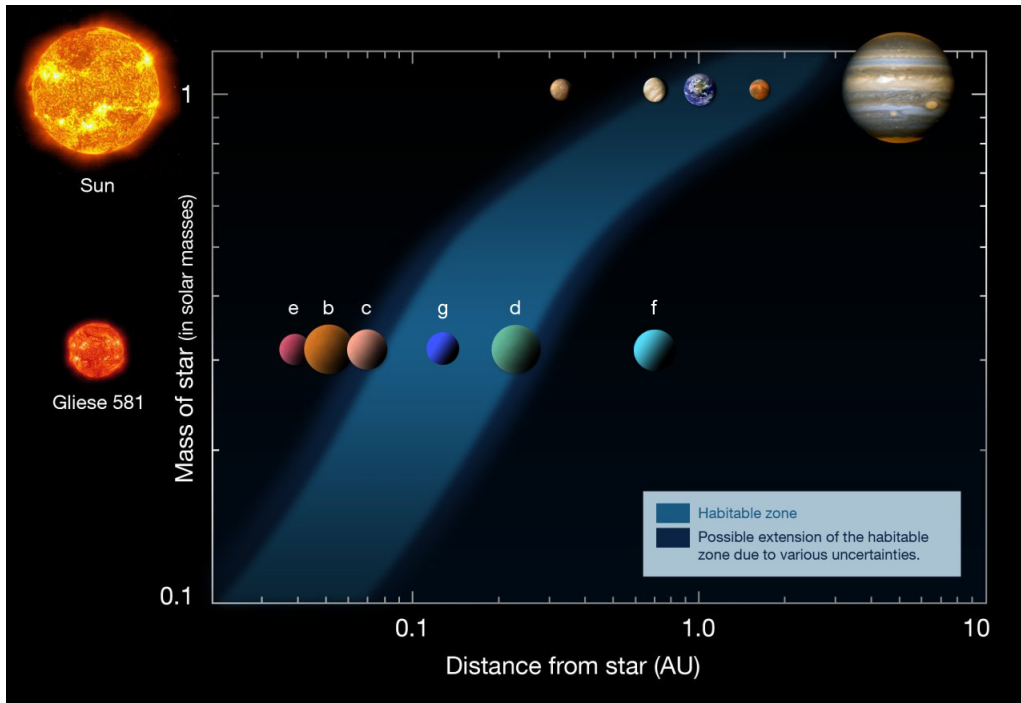


FIG. 3: The position of the habitable zone as a function of the star radius. Gliese 581g, although by far the best candidate, was dis-confirmed being an exoplanet in 2014. Gliese 581d remains the best candidate. (Image credit: European Southern Observatory.)

### III. HOW TO FIND EXOPLANETS? OVERVIEW OF THE PHOTOMETRIC METHODS

Exoplanets are tiny celestial bodies which may be difficult to observe directly, although direct imaging methods are used<sup>26</sup>. Instead, and this is a brilliant cornerstone in this domain of research, one may observe an exoplanet indirectly by the effect it has on its host-star. The variations in the light flux from stars can be studied and inferences can be made on the possible existence and characteristics of nearby orbiting objects.

#### A. Radial velocity

As always, in astronomy, or more generally speaking in physics, one needs a set of coordinates to describe a moving object. It is a matter of tradition that the line of sight by which an observer on Earth will look upon a distant star is defined as being the z-axis<sup>27</sup>, which therefore suggests that the plane of the sky is the x-y plane.

The radial velocity method gives the best results in the very restricted case where the z-axis (the line of sight) lies within the orbital plane of the exoplanet around the host-star (or at least when it is approximately the case), such that the angular momentum of the exoplanet is perpendicular to the z-axis. It is based on the following: when one looks at a star with, for instance, one orbiting exoplanet, one might “see” (this method of “seeing” will be explained later) that the star is actually moving along the line of sight, slightly closer to Earth, then further away and then closer again. This is explained by the fact that the exoplanet and the host-star are orbiting their common center of mass (CM) as shown on Figure 4.

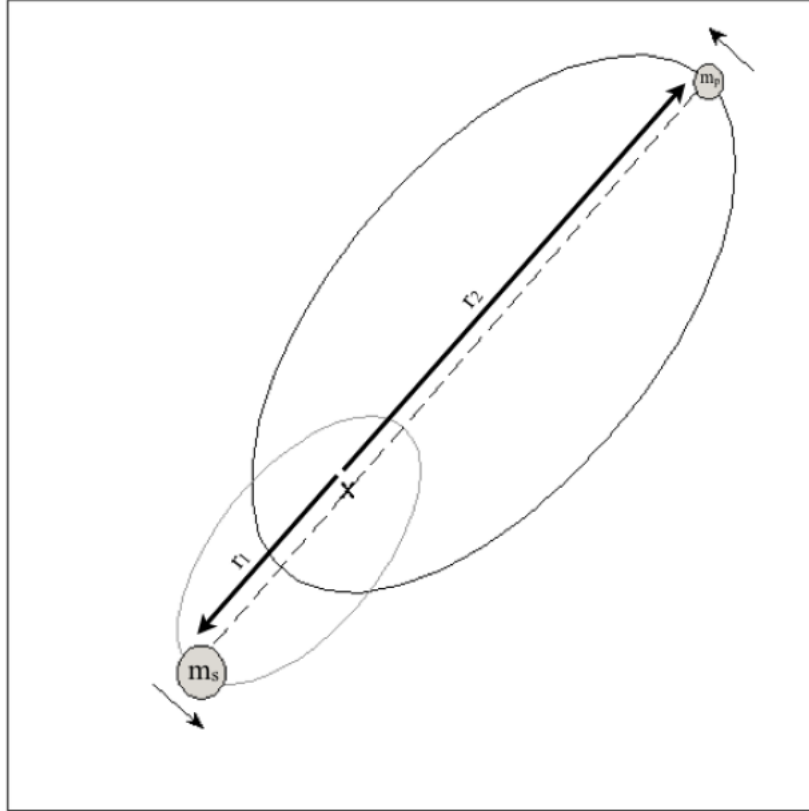


FIG. 4: An exoplanet of mass  $m_p$  and its host star of mass  $m_s$ , orbiting in opposite direction at a distance  $r_2$  and  $r_1$ , respectively, from a common center of mass denoted by “X” (as shown by the two smaller black arrows). (Image credit: Placek B. (2014). “Bayesian Detection and Characterization of Extra-Solar Planets Via Photometric Variations”. Dissertation, ProQuest/UML.)

One is intuitively drawn to think that if one were to look at the solar system from a nearby star, one would see the sun fixed or moving at a constant velocity in space with the planets orbiting around. It is indeed very much the case but, in fact, one would look at the only point in space moving with a constant uniform velocity, the CM, and one would find herself or himself in the frame of reference of the CM. The CM of the solar system is very close to the center of the Sun (it actually lies within its radius), but if one had instruments powerful enough, one would see from her or his distant star that the Sun is in fact revolving (wobbling) around the CM.

Formally, coming back to the single exoplanet system example described above (but the same reasoning would apply to any number of planets), the following mathematics can be used: the center of mass is defined as<sup>28</sup>:

$$\mathbf{R} = \frac{m_s \mathbf{r}_s + m_e \mathbf{r}_e}{m_s + m_e}, \quad (1)$$

where  $m_s$  and  $r_s$  stand for the mass and the radius of the star, respectively, and where  $m_e$  and  $r_e$  stand for the mass and the radius of the orbiting exoplanet. For convenience, if the coordinate system is now placed at the CM ( $R = 0$ ), it is then obtained that:

$$m_s \mathbf{r}_s = -m_e \mathbf{r}_e, \quad (2)$$

which says that the exoplanet and its host-star are orbiting the CM in opposite directions. Now, letting  $M = m_s + m_e$  be the total mass of the system, (1) can be rewritten as:

$$M \mathbf{R} = m_s \mathbf{r}_s + m_e \mathbf{r}_e, \quad (3)$$

and then taking the derivative on both sides of (3), it is obtained that:

$$M \dot{\mathbf{R}} = m_s \dot{\mathbf{r}}_s + m_e \dot{\mathbf{r}}_e = \mathbf{P}, \quad (4)$$

where  $\mathbf{P}$  is the total momentum of the system. In other words, the two-body problem reduces to that of one body of mass  $M$  with velocity equal to that of the CM. It is a remarkable and well-known result in classical mechanics<sup>28</sup>. If it is assumed that the total momentum is conserved (the system is not under the influence of an external force), then  $\dot{\mathbf{R}}$  is constant. One becomes free to choose a frame where the CM is at rest, which is particularly convenient to analyze the motion.

It can be seen that the motion of the star along the line of sight is therefore dependent upon the characteristics of the orbiting exoplanet(s). Knowing this, the question is what is meant when it is said that one “sees” the motion of a star? One uses, in fact, the Doppler effect (or Doppler shift) perceptible in the light coming from the star and which is schematically represented on Figure 5. As the star is moving closer to the Earth, the light wavelength as received by the observer decreases, its frequency therefore increases and the light is hence blue-shifted. Conversely, as the star is receding, the light wavelength increases, its frequency decreases and the light is red-shifted<sup>29</sup>.



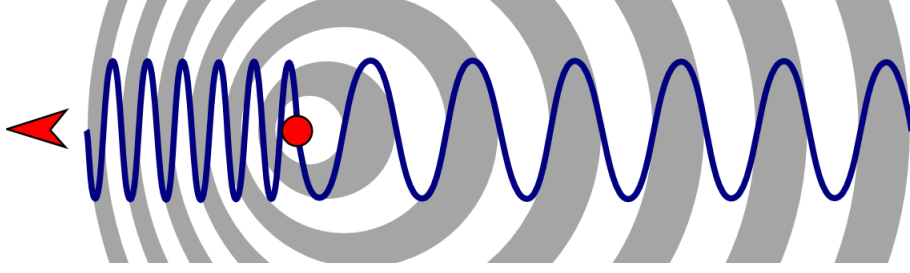


FIG. 5: The star is shown as the red dot. As it is moving in the direction pointed by the red arrow, the light is blue-shifted. Conversely, as it is moving in the direction opposite the red arrow, the light is red-shifted. (Image credit: released into the public domain by User:Antilived (2006). *Doppler effect (diagrammatic)*. Wikimedia Commons)

Figure 5 makes it evident to see why the redshift  $z$  is defined as<sup>29</sup>:

$$z = \frac{\lambda_{obs} - \lambda_{em}}{\lambda_{em}}, \quad (5)$$

where  $\lambda_{obs}$  is the observed wavelength coming from the star and  $\lambda_{em}$  is the emitted wavelength. It should be noted that formula (5) does not take into account relativistic effects since the radial velocities of stars is on the order of  $10^2$  to  $10^3$  m/s, it is acceptable to ignore them<sup>29</sup>.

Despite its success (it led to the discovery of the exoplanet 51 Pegasi b in 1995), the radial velocity method has limitations: it implies that the star, the planet and the observer on Earth have to be aligned for the method to yield satisfactory results. A planet that is orbiting its host-star with a small inclination relative to the plane of the sky has very little chance to be detected using this method, much less to be attributed correct characteristics regarding its mass or eccentricity<sup>27</sup>. Its radius is also impossible to determine. Finally, the planet has to have sufficient mass in order for the host-star to orbit sufficiently far from the CM, so that the resulting Doppler effect becomes measurable. This method is therefore biased against smaller, less massive planets. This is why it is today used as a confirmation rather than as a primary method of discovering extra-solar systems<sup>27</sup>. The next photometric effects to be discussed are however much more useful and precise.

## B. The transit method

Let's consider again a single exoplanet orbiting its host-star. In the very peculiar instance where the planet, the observer and the host-star are aligned with each other, but where the radial velocity method cannot be used effectively, one can use the fact that the planet will transit in front of the host-star. During the resulting eclipse (called the *primary* eclipse<sup>27</sup>) the light received from the star is slightly dimmed, which becomes apparent to the observer. The Kepler observatory is capable of such detections, which demonstrates the incredible degree of sophistication of its photometer.

A slightly more difficult physical observation to make is what astronomers refer to as the *secondary* eclipse<sup>27</sup>. The planet will not only transit in front of the host-star but, of course, it will also transit behind. As it is eclipsed by the host star, the associated drop in thermal energy (the energy radiated by the planet by virtue of its temperature) and in the reflected light are quantifiable. The eclipse depth  $\Delta F_p$  is calculated using:

$$\Delta F_p = \frac{T_d}{T_{eff}} \left( \frac{R_p}{R_s} \right)^2, \quad (6)$$

where  $T_d$  is the day-side temperature on the planet,  $T_{eff}$  is the effective temperature of the star respectively,  $R_p$  and  $R_s$  are the radius of the planet and of the star, respectively.

Geometric models can be made to estimate how the primary and secondary transits will affect the recording of the light flux through time. A typical orbital phase and the corresponding light curve is shown on Figure 6. The simplest of these models (consisting of the planet orbiting perfectly across the line of sight of the observer) results in a very sharp trough in the flux intensity for both the primary and secondary transit (the magnitude of the dip is less for the secondary transit).

However, in reality, stars are brighter near their center and dimmer toward their limbs. If the planet transits closer to the limbs, the resulting limb-darkening effect must be taken into account where the flux intensity decreases more smoothly and becomes more gradual<sup>27</sup>.

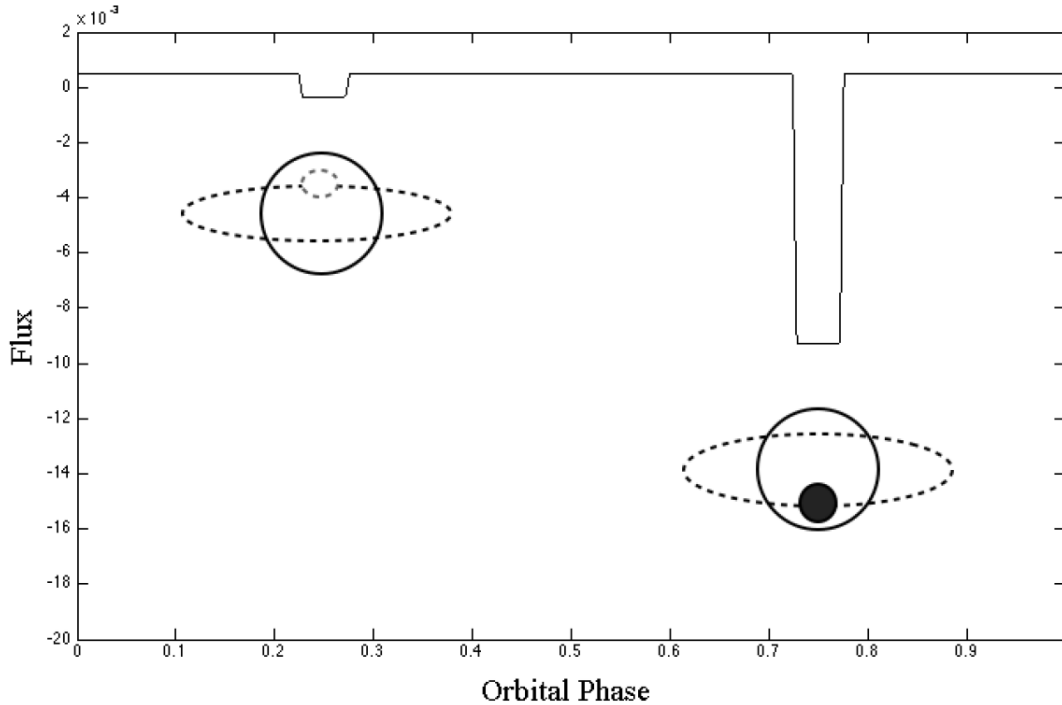


FIG. 6: As the planet orbits around its host-star, it will periodically decrease the light flux received on Earth when it transits in front of the star (primary eclipse). As the planet passes behind the star (secondary eclipse), the reflected and thermal radiations will be missing from the overall recorded flux, giving rise to a secondary, however smaller, dip in the light curve. (Image credit: Placek B. (2014). “Bayesian Detection and Characterization of Extra-Solar Planets Via Photometric Variations”. Dissertation, ProQuest/UMI.)

As one might expect, the limitations of this method again revolve around the fact that the transit of an exoplanet around its host star is an extremely rare event. It implies the relatively perfect alignment of the exoplanet, the host star and the observer. Since stars appear almost as points of light to an observer, even the closest ones, the apparent solid angle they occupy remains extremely small<sup>27</sup>. As we mentioned before, Kepler is surveying approximately 145000 stars. The total number of candidates and confirmed exoplanets is currently around 6000<sup>11</sup>. This brings the probability that a star has at least one transiting exoplanet to only 4%.

One can also calculate the transit probability  $P_t$ , which is a measure of how likely one is to find a star with a transiting exoplanet, given that *a priori* the orientation of the orbit is completely arbitrary. One can find  $P_t$  using<sup>27</sup>:

$$P_t = \frac{R_s}{a}, \quad (7)$$

where  $a$  is the orbital radius. As an example, if the radius of the Sun is used for  $R_s$  and the radius of the Earth's orbit for  $a$ , it is found that  $P_t$  is about 0.46%<sup>27</sup>, which is the probability of detecting an Earth transit from another star system. One sees therefore the necessity to develop new tools for finding non-transiting exoplanets, as transiting ones are but a tiny part of the extrasolar planetary population.

### C. Reflected light

Under the assumption that a star radiates isotropically, one can study variations in the light curves from the Kepler data under the further assumption that those variations are due to some of the light being reflected by an exoplanet. The power of this method lies in the fact that there is no need for a transit. Typically, a Lambertian model is assumed to describe the reflectance of a planet, which is a relatively crude but valid approximation to use<sup>27</sup>.

In Lambertian reflectance, in addition to isotropy, the reflecting surface is assumed to obey the Lambert's cosine law, which states that a surface element radiates with an intensity proportional to the cosine of the angle between the observer and the normal<sup>30</sup>, as shown on Figure 7.

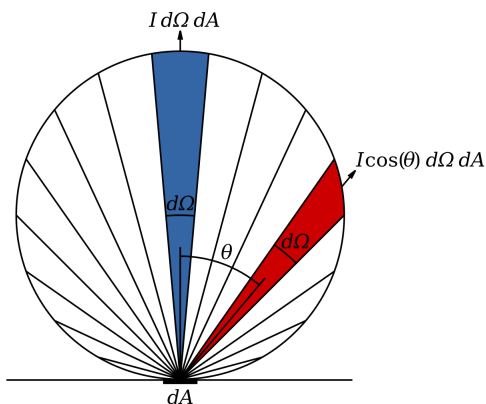


FIG. 7: This diagram shows a small surface  $dA$  radiating through a solid angle  $d\Omega$  according to Lambert's cosine law;  $I$  represents the radiance and decreases as then angle  $\theta$  increases between the normal to  $dA$  (the middle of the blue wedge) and the observer (observing through the red wedge). (Image credit: released into the public domain by User:Wchargin (2015).

*Lambert Cosine Law*. Wikimedia Commons)

In mathematical terms, Lambert’s law is stated as:

$$F_\theta = F_0 \cos(\theta), \tag{8}$$

where  $F_\theta$  is the reflected luminous intensity (or flux) at an angle  $\theta$  and  $F_0$  is the intensity just above the emitting surface ( $\theta = 0$ ). Let’s now try to find the luminosity,  $L_p$ , of a planet. By definition, the luminosity is nothing more than the intensity multiplied by the emitting surface area. In the case of an infinitesimally small surface element,  $dA$ , we have:

$$dL_p = F_\theta dA, \tag{9}$$

which, using (8), becomes:

$$dL_p = F_0 \cos(\theta) dA. \tag{10}$$

To express  $F_0$  in terms of the incident stellar flux,  $F_s$ , one can use the fact that the planet will not reflect the light entirely: the effective albedo,  $A_{eff}$ , must be taken into account, which is a measure of the “capacity” of the planet to reflect or absorb light from the host-star. By definition:

$$A_{eff} = \frac{F_0}{F_s}, \tag{11}$$

and hence:

$$F_0 = A_{eff} F_s. \tag{12}$$

Substituting (12) into (10), we obtain an expression for  $dL_p$ :

$$dL_p = A_{eff} F_s \cos(\theta) dA. \tag{13}$$

To obtain  $L_p$ , one has to integrate over the entire reflecting surface visible from the line of sight, which varies through time. Mathematically, it means that  $\theta$  is dependent upon time:  $t$ . For the sake of clarity, the complete derivation is not reproduced here and only the result will be quoted, but if one carries out the integration, one can find that<sup>27</sup>:

$$L_p(t) = \frac{A_{eff} F_s \pi R_p^2}{2} (1 + \cos \theta(t)). \tag{14}$$

One can use the fact that  $F_s$  is related to the stellar luminosity  $L_s$  by:

$$F_s = \frac{L_s}{4\pi r(t)^2}, \quad (15)$$

where  $r(t)$  expresses the fact that the separation between the planet and the host-star can be varying (the orbit is expected to be eccentric in most cases rather than perfectly circular). Hence, equation (14) becomes:

$$\frac{L_p(t)}{L_s} = \frac{A_{eff}}{8} \left( \frac{R_p}{r(t)} \right)^2 (1 + \cos \theta(t)). \quad (16)$$

One can also express the planetary flux,  $F_p$ , received at Earth across a distance  $d$  (which can be approximated as being constant through time) as<sup>27</sup>:

$$F_p = \frac{L_p}{4\pi d^2}. \quad (17)$$

Similarly, the stellar flux received at Earth is:

$$F_{se} = \frac{L_s}{4\pi d^2}. \quad (18)$$

Using (17) and (18) into (16), one can obtain the following relation for the normalized flux received at Earth due to reflected planetary light:

$$\frac{F_p(t)}{F_{se}} = \frac{A_{eff}}{8} \left( \frac{R_p}{r(t)} \right)^2 (1 + \cos \theta(t)). \quad (19)$$

#### D. Thermal emission

As the orbiting planet receives radiation from the star, it will reflect part of it (which is described by the albedo effect) but it will also produce thermal radiation. When the temperature is above absolute zero, collisions between molecules and atoms constantly change their kinetic energy.

When the orbit is circular, it is virtually impossible, by analyzing the flux density of light, to determine which portion is due to thermal emission and which portion is due to reflectance, since both vary sinusoidally<sup>27</sup>. However, as the orbit becomes more eccentric,

the reflectance will start to significantly deviate from a perfect sinusoid.

To describe mathematically how the flux of the dayside thermal emission  $F_{TE,d}$  varies through time, one needs a relation between  $F_{TE,d}$  and the total flux  $F_p(T_d)$  from the dayside of the planet. The Lambertian model is again used to describe the dayside luminosity due to the thermal emission of a surface element,  $dL_{TE,d}$ . One has<sup>27</sup>:

$$dL_{TE,d} = F_p(T_d) \cos(\theta) dA, \quad (20)$$

and by integrating this last expression, one can find how the dayside luminosity varies through time:

$$L_{TE,d}(t) = \frac{F_p(T_d) \pi R_p^2}{2} (1 + \cos \theta(t)). \quad (21)$$

As always, to go from the luminosity  $L_{TE,d}$  to the flux  $F_{TE,d}$ , one uses:

$$F_{TE,d}(t) = \frac{1}{4\pi d^2} L_{TE,d} = \frac{F_p(T_d) \pi R_p^2}{8d^2} (1 + \cos \theta(t)). \quad (22)$$

Dividing both sides of (22) (or normalizing) by the stellar flux  $F_s$  and using the fact that  $L_s = F_s(\pi R_s^2)$ , the expression wanted between  $F_{TE,d}$  and the total flux  $F_p(T_d)$  is obtained:

$$\frac{F_{TE,d}(t)}{F_s} = \frac{1}{2} \left( \frac{R_p}{R_s} \right)^2 (1 + \cos(\theta(t))) \frac{F_p(T_d)}{F_s}. \quad (23)$$

Similarly, the nightside luminosity due to the thermal emission of a surface element,  $dL_{TE,n}$ , can be written as:

$$dL_{TE,n} = F_n(T_n) \cos(\theta - \pi) dA. \quad (24)$$

Following the same reasoning as above, one can write the nightside thermal emission  $F_{TE,n}$  in terms of the total flux  $F_p(T_n)$  from the nightside of the planet as:

$$\frac{F_{TE,n}(t)}{F_s} = \frac{1}{2} \left( \frac{R_p}{R_s} \right)^2 \left( 1 + \cos(\theta(t) - \pi) \right) \frac{F_p(T_n)}{F_s}. \quad (25)$$

Hence, the total thermal emission  $F_{TE}$  received at Earth is given by:

$$F_{TE}(t) = F_{TE,d}(t) + F_{TE,n}(t). \quad (26)$$

## E. Doppler boosting

As a star is moving closer to Earth along the line of sight or further away, due to its rotation around the CM as described above, there is another principle that affects the light flux received by the observer standing on Earth, which has to do with relativistic aberration of light. This effect is named Doppler boosting, it arises when the flux decreases due to the star moving away from Earth, and when it increases due to the star moving closer<sup>27</sup>. If the speed  $v$  of a star relative to the Earth is close to the speed of light  $c$ , then the Lorentz's transformations arising from Special Relativity between referential frames must be taken into account. In practice, however, one will see that  $v$  is sufficiently small with respect to  $c$  as to allow some approximations to be made.

The demonstration of the effect of Doppler boosting requires mathematical concepts and notions that are beyond the scope of this paper, however it can be shown that the flux  $F_{boost}(t)$  through time due to Doppler boosting can be computed using<sup>27</sup>:

$$F_{boost}(t) = F_s \left( \frac{1}{\gamma(1 - \beta \cos \theta(t))} \right)^4 \quad (27)$$

where  $\gamma = (1 - \beta^2)^{-1/2}$  and  $\beta = \frac{v}{c}$ , where  $v$  is the speed of the star relative to Earth and  $c$  is the speed of light. In this context,  $F_s$  is the stellar flux in the star frame of reference.

The radial velocities are usually in the order of  $10^2$  to  $10^3 m s^{-1}$  so that  $\beta$  is in the order of approximately  $10^{-5}$ . Hence, one can make the approximation that  $\gamma \approx 1$  and:

$$\frac{F_{boost}(t)}{F_s} = (1 - \beta \cos \theta(t))^{-4} \quad (28)$$

Using a binomial expansion on the right side of (28), it is obtained that:

$$\frac{F_{boost}(t)}{F_s} = 1 + 4\beta \cos \theta(t). \quad (29)$$

As can be seen, there is a relativistic effect of *time dilation* due to the star motion along the line of sight. To illustrate equation (29), Figure 8 shows the normal flux received from a star at rest and how the flux changes as the star is moving.



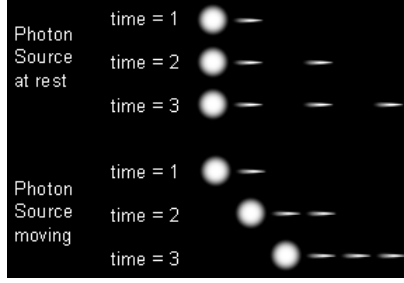


FIG. 8: Light can be conceived as a beam of particles (photons) having wavelike properties. When the star is at rest, photons are emitted at regular interval. When the star is moving, it is as if photons were emitted at different frequencies, modifying the flux accordingly (in this case, the luminosity appears to be brighter as photons are more densely “packed” together) which, in turns, induces a time dilation due to the speed of light,  $c$ , being taken as invariant in special relativity. (Image credit: released into the public domain by User:Mrbrak (Kollgaard, R) (2004). *Jet Dilation*. Wikimedia Commons).

## F. Ellipsoidal variations

The last photometric effect that has been generally taken into account so far in characterizing exoplanets, along with those described above, is called *ellipsoidal variation*. When a massive planet orbits close to its host-star, the gravitational tidal force due to the planet “distorts” the spherical shape of the star into a “prolate spheroid with the semi-major axis pointing approximately toward the planet”<sup>27</sup>. It results in a periodic fluctuation of the stellar flux as observed on Earth.

To model this effect perfectly is computationally expensive and offers little benefits<sup>27</sup>. Hence, approximations are often made and the following formula is commonly used to find the variations in flux  $F_{ellip}(t)$  through time due to the ellipsoidal variations of the star<sup>27</sup>:

$$\frac{F_{ellip}(t)}{F_s} = \beta \frac{M_p}{M_s} \left( \frac{R_s}{r(t)} \right)^3 [\cos^2(\omega + \nu(t)) + \sin^2(\omega + \nu(t)) \cos^2 i] \quad (30)$$

where  $M_p$  and  $M_s$  are the masses of the orbiting planet and of the star, respectively;  $R_s$  is the radius of the star and  $r(t)$  is the distance between the planet and the star;  $\nu(t)$  is called the true anomaly, it is the angle between the periapsis (the point where  $r(t)$  is minimum along the orbit) and the current position of the planet;  $i$  is the angle between the orbital plane and the plane of reference (by convention, the plane of the sky);  $\omega$  is the argument of the periastron (the point where  $r(t)$  is greatest). Among the most interesting param-

eters is  $\beta$ , which is a measure of the *gravity darkening effect* due to the ellipsoidal variations.

The following formula<sup>27</sup> gives a means to compute  $\beta$ :

$$\beta = \log \left( \frac{GM_s}{R_s^2} \right) (\log T_{eff})^{-1} \quad (31)$$

where  $G = 6.67 \times 10^{-11} Nm^2/Kg^2$  is the Gravitational constant and  $T_{eff}$  is the effective temperature of the star (the temperature at its surface). Physically,  $\beta$  arises from the fact that, as the star is “compressed” into an ellipsoid, the surface gravity becomes lower at the “equator” since it is further away from the center of the star. The effective temperature is therefore also affected and is lower in that area which, in turns, decreases the flux. To an observer on Earth, the equator (or the “bulges”) appears to be less bright than the poles<sup>27</sup>.

## IV. CHARACTERIZING EXOPLANETS: APPLYING BAYES' THEOREM IN THE ALGORITHM EXONEST

### A. Bayes' theorem

So far, in this paper, the most commonly used photometric effects have been considered. They constitute the scope of observations that one can make from “looking” at the stars, the raw data that comes from measurement. Now, however, the challenge is to deduce the characteristics of the extra-solar systems that can produce such data. More specifically, as it has been seen in the previous section, one can use mathematics to develop models of the light flux to explain the data from the different photometric effects. However, how is it known, specifically, which model is closest to describing the characteristics of the system?

To remedy this problem, statistical analysis seems to be among the most appropriate tools. In 1763, the solution to a problem of inverse probability (how to determine the probability distribution of an unobserved variable) was read in front of the Royal Society on behalf of the deceased Thomas Bayes<sup>31</sup>. The subsequent Bayes' theorem became a cornerstone of statistical theory. Mathematically, it can be expressed<sup>32</sup> as (where  $A$  and  $B$  are two events):

$$P(A|B) = \frac{P(A)P(B|A)}{P(B)}, \quad (32)$$

where  $P(A|B)$  is the probability of  $A$  given  $B$ ,  $P(B|A)$  is the probability of  $B$  given  $A$ , and  $P(A)$  and  $P(B)$  are respectively the probability of  $A$  and  $B$  happening, independently of each other. Hence, one has:

$$P(A|B) \propto P(B|A). \quad (33)$$

As can be seen from (33), the equation is “circular”, in the sense that it links the probability of the first event given the truth of the second event to the probability of the second event being true if the first event is realized. The power of that method, which seems relatively simple conceptually, is that one can infer models on the data being studied by analyzing instead how likely the data is explained by a particular model. We can rewrite Bayes' theorem in a slightly more “sophisticated” way to fit the case of data analysis<sup>32</sup>:

$$P(\theta_M|D, M) = \frac{P(\theta_M|M)P(D|\theta_M, M)}{P(D|M)}, \quad (34)$$

where  $M$  is the suggested model,  $\theta_M$  is the ensemble of parameter values associated with  $M$ , and  $D$  is the actual data. In that case,  $P(\theta_M|D, M)$  is called the *likelihood function*: it is a measure of the likelihood that  $M$ , and its associated set of parameters  $\theta_M$ , explain the data  $D$ . Conversely,  $P(\theta_M|M)$ , called the *posterior probability*, is a measure of what is known of  $M$  and  $\theta_M$  after considering  $D$ . The *evidence*,  $P(D|M)$ , is a measure of the likelihood that  $M$ , independently of the prior information, can explain  $D$ . Similarly, the *prior probability*,  $P(\theta_M|M)$ , represents what is known about  $M$  and  $\theta_M$  before considering the data  $D$ .

Again, as one can conclude from (34), Bayes' theorem, by its mathematical layout, takes what is known about a particular model and the probability that the model explains the data to “update” the probability that the data explains the model. Such circular, iterative reasoning, is easily handled by a computer.

It is interesting to note that the evidence is computed using the following equation<sup>27</sup>:

$$P(D|M) = \int P(\theta_M|M)P(D|\theta_M, M)d\theta_M, \quad (35)$$

where it can be seen that  $P(D|M)$  is, in fact, a “prior-weighted average of  $P(D|\theta_M, M)$ ”. From this equation, it appears that the more  $\theta_M$  is extended (the more parameters are taken into account or, in other words, the more complex the model appears to be), the lower the prior probability. Bayes' theorem has therefore the particularity to be in accordance with the Occam's Razor principle, which states that, from a set of hypotheses which all describe a set of data or experiments equally well, the hypothesis that makes the smallest number of assumptions shall be retained<sup>27</sup>.

## B. Multinest sampling

Using Bayesian methods, it is therefore possible to create an algorithm that “loops” until it matches the most probable set of model parameters to the actual data (in the case of the study of Exoplanets: the data obtained from the different photometric effects that have been discussed). The challenge in determining that particular model is time. In a multi-dimensional parameter space (i.e. when many different parameters shall be determined), converging to the solution can be, indeed, a very slow process. By solution, it is meant here to find the “best” combination of the parameters forming the space, so that the probability that the model defined by those parameters fits the data appropriately is maximized.

In order to apply Bayes’ theorem to the study of such parameter spaces, one method is “sampling”: to create samples (different models, each with a specific set of parameters) and select the one that best fit the data<sup>27</sup>. Unfortunately, to create many samples and to “jump” from one to the other in search of the “peak” (the maximum probability) can be incredibly slow.

One way to reduce this problem is to use model selection. It would be at one’s advantage to be able to gauge which model is more likely to describe the data than the other. The evidence, here, plays a crucial role. It can be shown<sup>33</sup>, using Bayes’ theorem, that:

$$R = \frac{P(M_1|\mathbf{D})}{P(M_2|\mathbf{D})} = \frac{P(M_1|\mathbf{D})P(M_1)}{P(M_2|\mathbf{D})P(M_2)} = \frac{Z_1 P(M_1)}{Z_2 P(M_2)}. \quad (36)$$

where  $M_1$  and  $M_2$  designate model one and model two. As can be seen, the ratio of the probability of the two models given the data is directly proportional to the ratio of the evidences  $Z_1$  and  $Z_2$ . In other words, being able to compare the evidences will allow for the selection of a preferred model.

Unfortunately, the task of computing the evidence can be daunting as well<sup>33</sup>. Nested sampling (NS) is an algorithm that uses a certain strategy to compute the evidence. It is beyond the scope of this paper to present a full description of NS, however, once the samples have been randomly generated (from the prior information), NS can compute the likelihood of each sample relative to the other, and discard the sample that has the worst

likelihood. From there, it will create a new sample, not from the prior information, but by copying a sample from the first set of randomly generated samples and proceed, yet again, by disregarding the worst sample. From there, by small increment, it will finally reach the set of highly probable models<sup>27</sup>.

It can encounter problems over a multimodal space (a space that contains several secondary “peaks” for the probability of the model fitting the data). In that case, the MultiNest algorithm can be used<sup>27</sup>. It essentially starts, as with NS, by creating samples and then it disregards the worst sample. The remaining samples are then sub-clustered into several multidimensional ellipsoids. MultiNest then searches for the finest solution inside those sub-clusters, essentially covering more space in less time. “More space” means that, in practice, it will encounter more secondary peaks per iteration, allowing it to map the topography of the space more quickly and efficiently toward the best solution. “Less time” means that the computation time can be reduced by 10 to 100 depending on the circumstances<sup>27</sup>.

## V. USING EXONEST TO CHARACTERIZE KEPLER-428B, 40B AND 44B

It is intended in this thesis to show that the algorithm Exonest, which uses MultiNest sampling, can efficiently determine exoplanets characteristics. To this end, three objects were selected, which are already confirmed exoplanets: Kepler 428b, 40b and 44b for which the parameters of interest (the planetary radius, its mass and its relative inclination) have already been estimated, independently, using different methodologies, thus offering the opportunity to compare the answers computed by Exonest. At the current stage of the algorithm development, it was deemed better to restrict the spectrum of choices, for each selection, to the case of a single hot Jupiter (one large planet orbiting relatively close to the star) for which the recorded “dip” in flux on the light curve is relatively important and clearly visible. Eventually, Exonest will be able to look at systems with multiple objects, large or small.

### A. Kepler-428b

The algorithm was run with an initial number of samples of 1000 using mainly the circular model. The values returned by Exonest for Kepler-428b are listed in Table I, as well as the values published on the NASA Exoplanet Archive<sup>34</sup> for comparison.

TABLE I: Kepler 428b: results given by Exonest and comparison with the published values.

Model	Number of samples	Parameters	Exonest	Uncertainty	NASA Exoplanet Archive	Uncertainty
Circular	1000	Inclination (°)	89.16	0.89	89.36	0.43
Circular	1000	Radius (in unit of Jupiter radius)	1.06740	$4 \times 10^{-5}$	1.08	0.03
Circular	1000	Mass (in unit of Jupiter mass)	4.23	0.17	1.27	0.19
Eccentric	100	Mass (in unit of Jupiter mass)	0.071	0.034	1.27	0.19
Circular	1000	Dayside temperature (°K)	2057.3	5.4	–	–
Circular	1000	Nightside temperature (°K)	890	260	–	–

As can be seen in Table I, the parameter values computed by Exonest are within uncertainties of the published values, except the mass. It was deemed interesting to add the estimates of the dayside and nightside temperatures on the planet. They seem reasonable but should be taken “cautiously” at this stage of Exonest development. As mentioned before, since the eccentricity of the orbit for Kepler-428b is estimated<sup>34</sup> to be less than 0.22, it might be difficult for the algorithm to determine which portion of the flux is due

to thermal emission and which portion is due to reflectance (they both vary sinusoidally as the planet orbits around the star). Hence, by not being able to untangle this information about the thermal emission, the algorithm is in a quandary as to the determination of the surface temperature.<sup>27</sup>.

The eccentricity might be source of confusion for the mass parameter as well. The result returned by the circular model is within 17 uncertainties of the value published on the NASA archive. The eccentric model was used to study that parameter only, and the computed value was only within two uncertainties. Again, the relative high eccentricity of 0.22 could be the cause of this problem. The fact that the eccentric model does not return a more accurate result is due to the number of samples used: 100 as opposed to a 1000 for the circular model. Unfortunately, the computation time is far longer for the eccentric than for the circular model, simply because the parameter space is more extended in the case of the eccentric model. It was difficult at this stage to go over 100 samples for this study, but it is expected that the algorithm will return more precise and accurate results as it is run with a higher number of samples.

A plot of the measured flux with respect to the phase was also created (Figure 9). It should be noted that, “by phase”, what is meant is the “folding” of several sets of measurements by the Kepler observatory. On the NASA Exoplanet Archive, the data is subdivided into “quarters” of observation, defined by a starting and an ending time. The duration of each observation depends on the type of “cadence”. A long cadence is defined as 29 minutes of observation, a short cadence is only 2 minutes long<sup>35</sup>. For instance, in the case of Kepler-428b, there are 17 long cadences but no short cadence available. By knowing the orbital period of the planet around the star, it is possible<sup>35</sup> to “fold” the cadences into each other to have several transits appearing on “top” of each other, effectively taking the average over several sets of measurements.



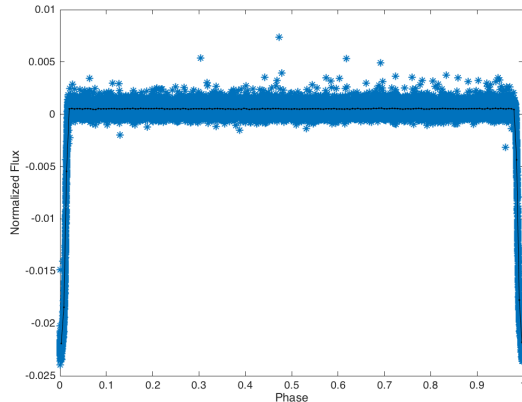


FIG. 9: Phase-folded light curve of Kepler-428b (in blue) with the binned time series (in black).

## B. Kepler-40b

Kepler-40b is another hot Jupiter-type planet orbiting close to its host star. It has an eccentricity of nearly zero<sup>34</sup> and it makes it a perfect candidate for the circular model. The analysis with Exonest was performed with 2000 samples to increase the precision. Results are listed in Table II.

TABLE II: Kepler-40b: results given by Exonest and comparison with the published values.

Model	Number of samples	Parameters	Exonest	Uncertainty	NASA Exoplanet Archive	Uncertainty
Circular	2000	Inclination ( $^{\circ}$ )	89.2985	$3.6 \times 10^{-3}$	89.7	0.3
Circular	2000	Radius (in unit of Jupiter radius)	1.20070	$3.2 \times 10^{-4}$	1.17	0.04
Circular	2000	Mass (in unit of Jupiter mass)	1.19	0.30	2.2	0.4

As can be seen in Table II, values are generally in agreement within one uncertainty of the published values, except for the relative inclination which is within five uncertainties. A possible source of error is the fact that it was necessary to perform a "data reduction". The data on the NASA archive is presented to the reader almost as it was recorded by the Kepler observatory, save the action of the *Kepler Presearch Data Conditioning* (which, in a recent update, also employs Bayesian techniques, to limit the impact of the noise on the measurements<sup>36</sup>), and it needs further treatment before it can efficiently be analyzed by Exonest.

As mentioned, the flux is recorded over several cadences of observation, but the flux might not be measured equally from one cadence to the next. It needs to be normalized around a common value of one. This process is not enough to guarantee the accuracy of the data. It needs to be “manually filtered” once again for any other systematic trend or stochastic error<sup>34</sup>, caused by the activity of the star itself (solar flares, for instance, will give sudden “spikes” on the light curve) or the drifting of the telescope, as shown on Figure 10. If the telescope drifts, the light from the star will move across the detectors, increasing the apparent brightness before the cadence stops, resulting in the light curve slightly increasing in intensity over time. Those trends are noise to Exonest and must be removed. In the process, of course, information about the planet and its characteristics are lost, resulting in less accuracy.

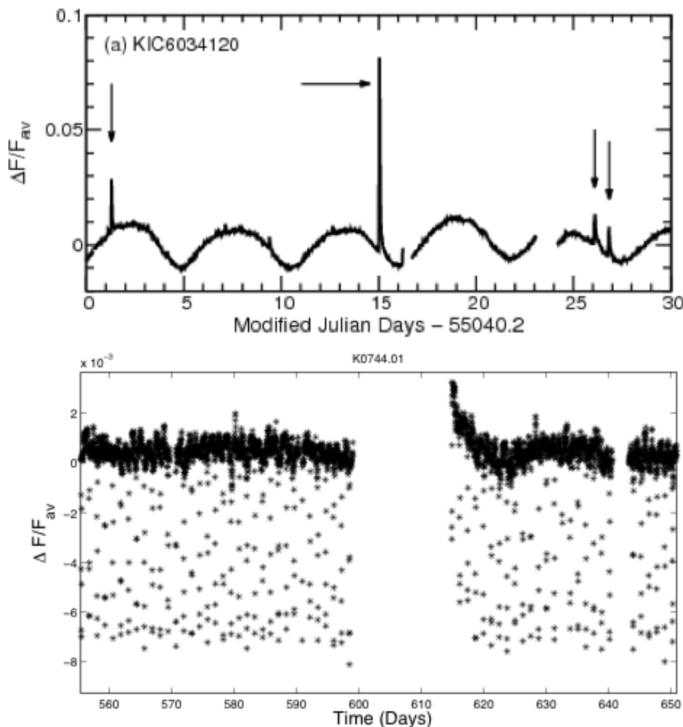


FIG. 10: On the top, the black arrows show spikes in the recorded flux due to solar flares. The bottom figure shows a gradual decrease in light flux with respect to time at the beginning of a new session of recording, which is due to the drifting of the telescope. (Image credit: Placek, B. (2015).)

Another source of error is the overall activity of the star (as opposed to specific events in its life, such as solar flares, as mentioned above). The light curve of Kepler-40b is shown in Figure 11. Outside the transition event, where the dip in the light flux occurs, it can

be seen that the star is very active in the sense that the normalized flux is “spread out” over a relatively large scale, especially when compared to Figure 9 for Kepler-428b. This is indicative of an active star and the secondary transit might be more difficult for Exonest to identify, leading to subsequent errors in the approximation of the orbit, and therefore of the mass.

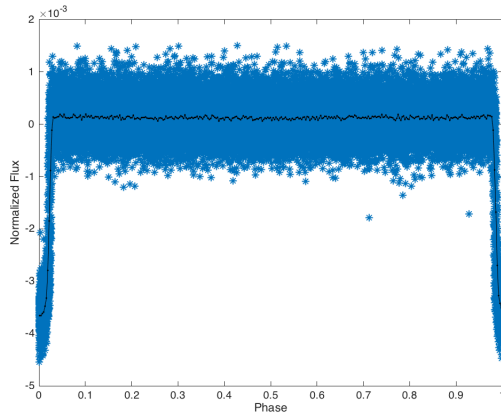


FIG. 11: Phase-folded light curve of Kepler-40b (in blue) with the binned time series (in black).

### C. Kepler-44b

The algorithm was run with 1000 samples, using the circular model as the eccentricity of Kepler-44b is only<sup>34</sup> of 0.066. The results are displayed in Table III.

TABLE III: Kepler-44b: results given by Exonest and comparison with the published values.

Model	Number of samples	Parameters	Exonest	Uncertainty	NASA Exoplanet Archive	Uncertainty
Circular	1000	Inclination ( $^{\circ}$ )	85.055	0.001	84.96	0.50
Circular	1000	Radius (in unit of Jupiter radius)	1.0768	$1 \times 10^{-4}$	1.09	0.07
Circular	1000	Mass (in unit of Jupiter mass)	0.72	0.13	1.00	0.10

As can be seen in Table III, the results regarding the inclination and the radius are within uncertainty of the published values. Only the mass seems to be slightly under-estimated by EXONEST: the result is within two uncertainties of the published value. This might be explained by the fact that the eccentricity is not perfectly zero, or this parameter might have been over-estimated by NASA as well. The sources of error previously mentioned for

Kepler-428b and 40b also apply. The light curve is shown in Figure 12 and it can be seen that the star is also very active in this case.

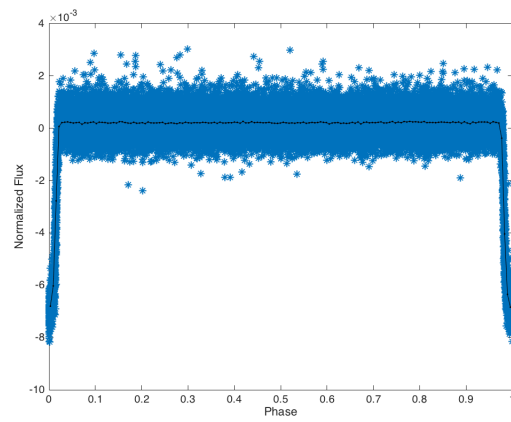


FIG. 12: Phase-folded light curve of Kepler-44b (in blue) with the binned time series (in black).

## VI. CONCLUSION

In this thesis, the algorithm Exonest, which was written for the analysis of the Kepler data, based on Bayesian methods, was tested in three cases. Three known confirmed exoplanets were studied: Kepler-428b, 44b and 40b for which characteristic parameters had already been estimated and published. Those parameters of interest were the relative inclination of the planet with respect to its host-star, its mass and its radius.

In the case of Kepler-428b, the values computed by Exonest were within uncertainty of the current published values, except the mass, which was calculated, using the eccentric model, to be within two uncertainties of the published value. A source of error was the relatively low number of samples used to save computation time. Regarding Kepler-40b, the parameters were again estimated within uncertainty of the published values, except the inclination, which was within five uncertainties. Several data reduction operations, which were performed to minimize the impact of the systematic trend due to the activity of the star (solar flares) or of the drifting of the Kepler observatory, were quoted as a possible sources of error. Finally, Kepler-40b was studied, and the parameters were computed within uncertainty of the published value, except the mass which was slightly under-estimated by Exonest. It was probably due to the sources of error previously mentioned.

Exonest is a promising tool in the search for exoplanets, and it is a good candidate to meet the challenges imposed by the ever increasing amount of data available. The algorithm, based on nested sampling, is fast and allows anyone having a regular home-based computer or laptop to analyze complex data. Future improvements include the capacity to use Exonest on several computers linked to a common server, to decrease the time necessary to perform computations. For now, the algorithm use has been limited to confirming the characteristics of hot Jupiters, orbiting close to their host-star. In the future, it will be possible to use Exonest with smaller planets, possibly in the habitable zone, to gain information on their features. It has also the potentiality to become a tool to identify objects of interest and promote them to the stage of confirmed exoplanets.

It seems interesting to conclude by coming back to the notion that the Universe has become vast, vaster than was thought even a century ago. According to our present knowledge of astronomy and astrophysics, it seems rather unlikely that life could have developed only on Earth or that humankind is the only intelligent species to be found across the emptiness of space. We might very well discover in the near future traces of an alien life, or we might not, raising, either way, profound philosophical questions regarding our place in the Universe.

We may have lost our privileged place at the center of Universe, we may lose our belief to be the only children of the Cosmos, we may lose our belief to be special, we may become afraid of finding ourselves drifting across infinite emptiness on a grain of sand. We might suffer from our loneliness and reclusion, or find the will to share with others in the beauties and harmonies of a multitude of Worlds. But that which we are, we are: ever since the dawn of consciousness that saw our ancestors making tools with their bare hands, human beings have “thought” the Universe in the sense that they have never ceased to apprehend the Cosmos with their own intelligence and sentience. They considered the Sun as a god traveling each day through the sky, then as a spherical body made of plasma, held by gravity, glowing from thermonuclear fusion between hydrogen atoms. The originality of that “thinking” is the product of a very specific combination of random and deterministic processes which took place during evolution, and were further shaped through history and culture. To imagine that this combination may be found again across the Universe is unlikely, unless the Universe is infinite and counts an infinite number of Worlds with copies of ours. They will most likely stay beyond reach. Hence, by trying to find meaningfulness to their lives, human beings are “thinking” the Universe, in a way that is specific to them, through art, science and dreams, with an increasing sophistication, and they will keep thinking the Universe in the future. That thinking is ours and will always be.

- 
- <sup>1</sup> Light from the stars falls quietly like rain. It does not make noise, it does not raise dust, it does not create wind. (*Translation by the author.*)
- <sup>2</sup> Shaw, G. J. (2014). *The Egyptian Myths: a Guide to the Ancient Gods and Legends*. Thames and Hudson, 2014. ISBN 978-0-500-25198-0.
- <sup>3</sup> Sagan, C. (1980). *Cosmos*. Ballantine Books Trade Paperbacks New York, 2013. ISBN 978-0-345-53943-4.
- <sup>4</sup> Bruno, G. (1584). *On the Infinite Universe and Worlds*.
- <sup>5</sup> Newton, Isaac; I. Bernard Cohen and Anne Whitman (1999) [1713]. *The Principia: A New Translation and Guide*. University of California Press. p. 940. ISBN 0-520-20217-1.
- <sup>6</sup> Wolszczan, A.; Frail, D. A. (1992). “A planetary system around the millisecond pulsar PSR1257 + 12”. *Nature* 355 (6356): 145.
- <sup>7</sup> Mayor, M.; Queloz, D. (1995). “A Jupiter-mass companion to a solar-type star”. *Nature* 378 (6555): 355.
- <sup>8</sup> National Aeronautics and Space Administration (2015). *NASA Aerospace Science and Technology Dictionary*. Retrieved August 20, 2015, from <http://www.hq.nasa.gov/office/hqlibrary/aerospacedictionary/508/508index.htm>.
- <sup>9</sup> National Aeronautics and Space Administration (2015). “Liftoff of the Kepler spacecraft”. Retrieved August 20, 2015, from [http://www.nasa.gov/mission\\_pages/kepler/launch/index.html](http://www.nasa.gov/mission_pages/kepler/launch/index.html).
- <sup>10</sup> National Aeronautics and Space Administration (2012). “The Milky Way’s 100 Billion Planets”. Retrieved August 20, 2015, from [http://www.nasa.gov/multimedia/imagegallery/image\\_feature\\_2233.html](http://www.nasa.gov/multimedia/imagegallery/image_feature_2233.html).
- <sup>11</sup> Dunbar, B.; Johnson, M. (2015). “How many exoplanets has Kepler discovered?”. National Aeronautics and Space Administration, 2015. Retrieved August 20, 2015, from <http://www.nasa.gov/kepler/discoveries>.
- <sup>12</sup> Johnson, M.; Harrington, J.D. (2014). “NASA’s Kepler Mission Announces a Planet Bonanza, 715 New Worlds”. National Aeronautics and Space Administration, 2014. Retrieved August 20, 2015, from <http://www.nasa.gov/ames/kepler/nasas-kepler-mission-announces-a-planet-bonanza>.

- <sup>13</sup> Schneider, J., Dedieu, C., Le Sidaner, P., Savalle, R., Zolotukhin, I. (2011). “Defining and cataloging exoplanets: the exoplanet. eu database”. *Astronomy & Astrophysics*, 532, A79.
- <sup>14</sup> Vorberger, J., Tamblyn, I., Militzer, B., Bonev, S. A. (2007). “Hydrogen-helium mixtures in the interiors of giant planets”. *Physical Review B*, 75(2), 024206.
- <sup>15</sup> Dumusque, X., Pepe, F., Lovis, C., Sgransan, D., Sahlmann, J., Benz, W., Bouchy, F., Mayor, M. et al. (2012). “An Earth mass planet orbiting Alpha Centauri B”. *Nature* 490 (7423): 20711.
- <sup>16</sup> Battersby, S. (2009). “Smallest known exoplanet may actually be Earth-mass”. *New Scientist*. Retrieved August 26, 2015 from <https://www.newscientist.com/article/dn16439-smallest-known-exoplanet-may-actually-be-earth-mass/>
- <sup>17</sup> Sahlmann, J., Lazorenko, P. F., Sgransan, D., Martín, E. L., Queloz, D., Mayor, M., Udry, S. (2013). “Astrometric orbit of a low-mass companion to an ultracool dwarf”. Harvard University.
- <sup>18</sup> Setiawan, J., Klement, R. J., Henning, T., Rix, H. W., Rochau, B., Rodmann, J., Schulze-Hartung, T. (2010). “A giant planet around a metal-poor star of extragalactic origin”. *Science*, 330(6011), 1642-1644.
- <sup>19</sup> Boudry, M., Blancke, S., Braeckman, J. (2010). “Irreducible Incoherence and Intelligent Design: A Look into the Conceptual Toolbox of a Pseudoscience”. *The Quarterly Review of Biology* 85 (4): 47382.
- <sup>20</sup> Forrest, B., Gross, P. R. (2007). *Creationism’s Trojan horse: The wedge of intelligent design*. Oxford University Press. ISBN 978-0195319736.
- <sup>21</sup> Coppens, Y., Picq, P. (2002). *Aux origines de l’humanité : Tome 2, Le propre de l’homme*. Fayard. ISBN 978-2702848258.
- <sup>22</sup> Greene, B. (2011). *The Hidden Reality*. First Vintage Books Edition. ISBN 978-0-307-27812-8
- <sup>23</sup> Huggett, R. J. (1995). *Geocology: An Evolutionary Approach*. Routledge, Chapman & Hall. p. 10. ISBN 978-0-415-08689-9.
- <sup>24</sup> Kopparapu, R.K. (2013). “A revised estimate of the occurrence rate of terrestrial planets in the habitable zones around kepler m-dwarfs”. *The Astrophysical Journal Letters* 767 (1): L8.
- <sup>25</sup> Robertson, P., Mahadevan, S., Endl, M., Roy, A. (2014). “Stellar activity masquerading as planets in the habitable zone of the M dwarf Gliese 581”. *Science*. arXiv:1407.1049
- <sup>26</sup> Rameau, J., Chauvin, G., Lagrange, A. M., Boccaletti, A., Quanz, S. P., Bonnefoy, M., M., Girard, J.H., Delorme, P., Desidera, S., Klahr, H. and Mordasini, C. (2013). DISCOVERY OF A PROBABLE 4-5 JUPITER-MASS EXOPLANET TO HD 95086 BY DIRECT IMAGING-



Based on observations collected at the European Organisation for Astronomical Research in the Southern Hemisphere, Chile, under program Nos. 087. C-0292, 088. C. 0085, 090. C-0538, 090. C-0698, and 090. C-0728. *The Astrophysical Journal Letters*, 772(2), L15.

- <sup>27</sup> Placek, B. (2014). “Bayesian Detection and Characterization of Extra-Solar Planets Via Photometric Variations”. Dissertation, ProQuest/UMI.
- <sup>28</sup> Taylor, J.R. (2005). *Classical Mechanics*. University Science Books. ISBN 978-1-891389-22-1
- <sup>29</sup> Liddle, A. (2003). *An Introduction to Modern Cosmology* (2<sup>th</sup> ed.). Wiley. ISBN 978-0-470-84835-7
- <sup>30</sup> Warren, J.S. (2007). *Modern Optical Engineering* (4<sup>th</sup> ed.). McGraw-Hill Education. ISBN 978-0071476874
- <sup>31</sup> Mr. Bayes, Mr. Price (1763). “An Essay towards Solving a Problem in the Doctrine of Chances. By the Late Rev. Mr. Bayes, F. R. S. Communicated by Mr. Price, in a Letter to John Canton, A. M. F. R. S.”. *Philosophical Transactions* (1683-1775), 53, 370-418. Retrieved January 22, 2016 from <http://www.jstor.org/stable/105741>.
- <sup>32</sup> Sivia, D. S., Skilling J. (2006). *Data analysis: a Bayesian tutorial* (2<sup>th</sup> ed.). Oxford university press. ISBN 978-0-19-856832-2.
- <sup>33</sup> Feroz, F., Hobson, M. P., Cameron, E., Pettitt, A. N. (2013). “Importance nested sampling and the MultiNest algorithm”. *arXiv preprint arXiv:1306.2144*.
- <sup>34</sup> NASA Exoplanet Archive. (n.d.). Retrieved February 05, 2016, from <http://exoplanetarchive.ipac.caltech.edu/>.
- <sup>35</sup> Placek, B. (private communication).
- <sup>36</sup> Stumpe, M. C., Smith, J. C., Van Cleve, J. E., Twicken, J. D., Barclay, T. S., Fanelli, M. N., ... & Morris, R. L. (2012). “Kepler presearch data conditioning I - Architecture and algorithms for error correction in Kepler light curves.” *Publications of the Astronomical Society of the Pacific*, 124(919), 985.